Theoretical Studies on O-Insertion Reactions of Nitrous Oxide with Ruthenium Hydride Complexes

Haizhu Yu, Guochen Jia,* and Zhenyang Lin*

Department of Chemistry, The Hong Kong University of Science and Technology, Clear Water Bay, Kowloon, Hong Kong, People's Republic of China

Received January 31, 2008

DFT calculations have been carried out to study the mechanism of the N_2O O-insertion into the Ru−H bonds of ruthenium hydride complexes $(dmpe)_2Ru(H)(X)$ (X = OH, H). The reaction pathways for the formation of the monoinsertion product $(dmpe)_2Ru(H)(OH)$ and the bis(hydroxo) complex $(dmpe)_2Ru(OH)(OH)$, which were obtained directly from the reactions of N_2O with the ruthenium hydride complexes, have been investigated in detail. Focus has been made to understand how the kinetically inert N_2O is activated by the hydride complexes. It is found that N_2O is activated through the hydride ligand nucleophilically attacking the terminal nitrogen of N_2O followed by coordination of the activated N_2O via the O-end.

Introduction

Nitrous oxide (N_2O), a chemically very inert molecule, has been increasingly recognized to play a harmful role in our environment, contributing to the greenhouse effect and ozone layer depletion. As a result, there has been growing interest in developing chemistry and catalysis that are relevant to the control of N_2O emission. Over the last few decades, a large number of reactions between transition metal complexes and nitrous oxide (N_2O) were reported. For example, reactions of transition metal complexes with N_2O to give the terminal/bridged metal-oxide or oxo products were reported.[1,2] Insertion of the N_2O oxygen into an M−C or M−H bond was studied.[3–6] Nitrous oxide N−N or N−O bond cleavage reactions were also found in molybdenum and osmium complexes.[7–9] Transition metal-catalyzed reactions of organic compounds with N_2O have been actively explored.[10,11] However, the mechanisms, which are important in designing metal complexes to activate N_2O, are not well studied. We recently theoretically investigated the reactions of N_2O with $Cp_2M(\eta^2$-alkyne) (M = Ti, Zr), reported in the 1990s by Hillhouse et al.[12,13] We showed that $Cp_2M(\eta^2$-alkyne) (M = Ti, Zr) activated N_2O by switching the metal(d)-to-alkyne(π^*) back-bonding interaction to a metal(d)-to-$N_2O(\pi^*)$ back-bonding interaction in $Cp_2M(\eta^2$-alkyne)(N_2O). In the transition state structures, the metal(d)-to-$N_2O(\pi^*)$ back-bonding interaction is maximized and the N end-on N_2O ligand carries a charge of −2, allowing the coordinated N to be electron-rich

* Corresponding authors. E-mail: chjiag@ust.hk; chzlin@ust.hk.

(1) For example: (a) Chadeayne, A. R.; Wolczanski, P. T.; Lobkovsky, E. B. *Inorg. Chem.* **2004**, *43*, 3421. (b) Veige, A. S.; Slaughter, L. M.; Lobkovsky, E. B.; Wolczanski, P. T.; Matsunaga, N.; Decker, S. A.; Cundari, T. R. *Inorg. Chem.* **2003**, *42*, 6204. (c) Baranger, A. M.; Hanna, T. A.; Bergmann, R. G. *J. Am. Chem. Soc.* **1995**, *117*, 10041. (d) Howard, W. A.; Parkin, G. *J. Am. Chem. Soc.* **1994**, *116*, 606. (e) Smith III, M. R.; Matunaga, P. T.; Andersen, R. A. *J. Am. Chem. Soc.* **1993**, *115*, 7049. (f) Bottomley, F.; Chen, J.; MacIntosh, S. M.; Thompson, R. C. *Organometallics* **1991**, *10*, 906. (g) Bottomley, F.; Magill, C. P.; Zhao, B. *Organometallics* **1991**, *10*, 1946. (h) Berg, D. J.; Burns, C. J.; Andersen, R. A.; Zalkin, A. *Organometallics* **1989**, *8*, 1865. (i) Almond, M. J.; Downs, A. J.; Perutz, R. N. *Inorg. Chem.* **1985**, *24*, 275. (j) Bottomley, F.; Egharevba, G. O.; Lin, I. J. B.; White, P. S. *Organometallics* **1985**, *4*, 550. (k) Bottomley, F.; Paez, D. E.; White, P. S. *J. Am. Chem. Soc.* **1982**, *104*, 5651. (l) Bottomley, F.; Paez, D. E.; White, P. S. *J. Am. Chem. Soc.* **1981**, *103*, 5581. (m) Bottomley, F.; Lin, I. J. B.; White, P. S. *J. Am. Chem. Soc.* **1981**, *103*, 703. (n) Hall, K. A.; Mayer, J. M. *J. Am. Chem. Soc.* **1992**, *114*, 10402.

(2) Conry, R. R.; Mayer, J. M. *Inorg. Chem.* **1990**, *29*, 4862.

(3) (a) Matsunaga, P. T.; Hillhouse, G. L.; Rheingold, A. L. *J. Am. Chem. Soc.* **1993**, *115*, 2075. (b) Koo, K.; Hillhouse, G. L. *Organometallics* **1996**, *15*, 2669. (c) Koo, K.; Hillhouse, G. L.; Rheingold, A. L. *Organometallics* **1995**, *14*, 456. (d) Koo, K.; Hillhouse, G. L. *Organometallics* **1998**, *17*, 2924. (e) Matsunaga, P. T.; Mavropoulos, J. C.; Hillhouse, G. L. *Polyhedron* **1995**, *14*, 175.

(4) Vaughan, G. A.; Rupert, P. B.; Hillhouse, G. L. *J. Am. Chem. Soc.* **1987**, *109*, 5538.

(5) Bleeke, J. R.; Behm, R. *J. Am. Chem. Soc.* **1997**, *119*, 8503.

(6) (a) Kaplan, A. W.; Bergman, R. G. *Organometallics* **1997**, *16*, 1106. (b) Kaplan, A. W.; Bergman, R. G. *Organometallics* **1998**, *17*, 5072.

(7) (a) Cherry, J. P. F.; Johnson, A. R.; Baraldo, L. M.; Tsai, Y. C.; Cummins, C. C.; Kryatov, S. V.; Rybak-Akimova, E. V.; Capps, K. B.; Hoff, C. D.; Haar, C. M.; Nolan, S. P. *J. Am. Chem. Soc.* **2001**, *123*, 7271. (b) Laplaza, C. E.; Odom, A. L.; Davis, W. D.; Cummins, C. C.; Protasiewicz, J. D. *J. Am. Chem. Soc.* **1995**, *117*, 4999.

(8) Lee, J.-H. P. M.; Tomaszewski, J.; Fan, H.-J.; Caulton, K. G. *J. Am. Chem. Soc.* **2007**, *129*, 8706.

(9) (a) Lee, J. D.; Fang, W. P.; Li, C. S.; Cheng, C. H. *J. Chem. Soc., Dalton Trans.* **1991**, 1923. (b) Li, C. S.; Sun, K. S.; Cheng, C. H. *J. Chem. Soc., Dalton Trans.* **1992**, 1025. (c) Barrientos, C.; Ghosh, C. K.; Graham, W. A. G.; Thomas, M. J. *J. Organomet. Chem.* **1990**, *394*, C31. (d) Bottomley, F.; Darkwa, J. *J. Chem. Soc., Dalton Trans.* **1998**, 2505.

(10) (a) Lee, C. H.; Lin, T. S.; Mou, C. Y. *J. Phys. Chem. C* **2007**, *111*, 3873. (b) Zhang, Q.; Guo, Q.; Wang, X.; Shishido, T.; Wang, Y. *J. Catal.* **2006**, *239*, 105. (c) Sehested, J. *Catal. Today* **2006**, *111*, 103. (d) Hensen, E. J. M.; Zhu, Q.; Janssen, P. A. J.; Magusin, P. C. M. M.; Kooyman, P. J.; van Santen, R. A. *J. Catal.* **2005**, *233*, 123. (e) Costine, A.; O'Sullivan, T.; Hodnett, B. K. *Catal. Today* **2005**, *99*, 199. (f) Ohtani, B.; Takamiya, S.; Hirai, Y.; Sudoh, M.; Nishimoto, S.; Kagiya, T. *J. Chem. Soc., Perkin Trans. 2* **1992**, 175. (g) Hashimoto, K.; Kitaichi, Y.; Tanaka, H.; Ikeno, T.; Yamada, T. *Chem. Lett.* **2001**, 922. (h) Yamada, T.; Hashimoto, K.; Kitaichi, Y.; Suzuki, K.; Ikeno, T. *Chem. Lett.* **2001**, 268. (i) Hashimoto, K.; Tanaka, H.; Ikeno, T.; Yamada, T. *Chem. Lett.* **2002**, 582. (j) Ben-Daniel, R.; Weiner, L.; Neumann, R. *J. Am. Chem. Soc.* **2002**, *124*, 8788. (k) Ben-Daniel, R.; Neumann, R. *Angew. Chem., Int. Ed.* **2003**, *42*, 92.

(11) (a) Yamamoto, A.; Kitazume, S.; Pu, L. S.; Ikeda, S. *J. Am. Chem. Soc.* **1971**, *93*, 371. (b) Arzoumanian, H.; Nuel, D.; Sanchez, J. *J. Mol. Catal.* **1991**, *65*, L9. (c) Yamada, T.; Suzuki, K.; Hashimoto, K.; Ikeno, T. *Chem. Lett.* **1999**, 1043.

(12) (a) Vaughan, G. A.; Hillhouse, G. L.; Rheingold, A. L. *J. Am. Chem. Soc.* **1990**, *112*, 7994. (b) Vaughan, G. A.; Sofield, C. D.; Hillhouse, G. L. *J. Am. Chem. Soc.* **1989**, *111*, 5491. (c) Vaughan, G. A.; Hillhouse, G. L.; Lum, R. T.; Buchwald, S. L.; Rheingold, A. L. *J. Am. Chem. Soc.* **1988**, *110*, 7215. (d) List, A. K.; Koo, K.; Rheingold, A. L.; Hillhouse, G. L. *Inorg. Chim. Acta* **1998**, *270*, 399.

(13) Yu, H.; Jia, G.; Lin, Z. *Organometallics* **2007**, *26*, 6769.

10.1021/om8000845 CCC: $40.75
Publication on Web 07/01/2008

Scheme 1

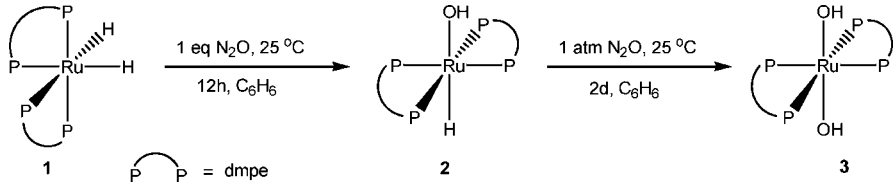

enough to nucleophilically attack the weakly bound alkyne ligand, to give four-membered metallacycle intermediates.

Continuing the effort to understand how metal complexes can activate N_2O,[13–15] we extend our research to reactions with late transition metal complexes. One of these reactions is the O-insertion reactions of N_2O with ruthenium hydride complexes reported by Bergman et al. (Scheme 1).[6] It was shown that treatment of the ruthenium dihydride **1** (dmpe = $Me_2P(CH_2)_2PMe_2$) with 1 equiv of N_2O afforded the hydroxoruthenium complex **2** in 41% yield after crystallization. Treatment of either the ruthenium dihydride **1** or the isolated monoinsertion product **2** with an atmosphere of N_2O afforded the bis(hydroxo) complex $(dmpe)_2Ru(OH)_2$ (**3**) in 30% yield.

The reaction reported by Bergman et al. shown in Scheme 1 represents the first example of oxygen atom transfers from N_2O to a late transition metal−hydride bond. It was proposed that the oxygen transfer proceeded through an N_2O-coordinated intermediate, shown in Scheme 2.[6] The proposed mechanism reflects traditional thinking that N_2O can be activated through coordination of N_2O to the metal center via the N- or O-end. In this paper, we report our theoretical investigation on the reaction mechanism for the reaction shown in Scheme 1. We hope that the insight provided through this study will help to design new systems for the activation of N_2O.

Computational Details

Molecular geometries of all the complexes studied were optimized without constraints via DFT calculations using the Becke3LYP (B3LYP) functional.[16] Frequency calculations at the same level of theory were also performed to identify all the stationary points as minima (zero imaginary frequencies) or transition states (one imaginary frequency) and to provide free energies at 298.15 K. Transition states were located using the Berny algorithm. Intrinsic reaction coordinates (IRC)[17] were calculated for the transition states to confirm that such structures indeed connect two relevant minima. The 6-311++G** Pople basis set[18] was used for O and N atoms and for those H atoms bonded to the metal center in the dihydride complex **1**. The SDDALL basis set[19] with Stuttgart potentials was used to describe Ru and P atoms. Polarization functions were also added for Ru (ζ(f) = 1.235) and P (ζ(d) = 0.340).[20] The 6-31G basis set was used for all other atoms. To examine the solvent effect, we also employed a continuum medium to do single-point calculations for several selected species, using the self-consistent reaction field (SCRF) based on the polarizable continuum model (PCM).[21] Benzene was used as solvent, corresponding to the experimental conditions. The results show that the solvent effect is very small. For example, without the solvation energies, the relative electronic energies of **2** and **3** with respect to **1** + N_2O (Scheme 1) are −63.8 and −125.2 kcal/mol, respectively. Considering the solvation energies, the relative electronic energies are −65.6 and −127.5 kcal/mol, respectively. Molecular orbitals obtained from the B3LYP calculations were plotted using the Molden 3.7 program written by Schaftenaar.[22] All the DFT calculations were performed with the Gaussian 03 package.[23] The natural bond orbital (NBO) program,[24] as implemented in Gaussian 03, was also used to obtain natural populations of atoms.[25]

Results and Discussion

Formation of 2 via N- or O-Coordination. We first examined the mechanism proposed in Scheme 2 by calculating the energetics for the formation of the intermediate **4a** involving coordination of N_2O to the metal center via the terminal N atom. Our calculations show that the linear conformation in **4a** proposed in Scheme 2 does not correspond to a local minimum. The results are understandable, as there would be formally 20 electrons around the metal center. Instead, we located the minimum structure **4a′** (Scheme 3), which can be considered as a nonclassical dihydrogen complex that has a dihydrogen ligand and contains a Ru(η^2-H_2) structural unit. Scheme 3 shows the relative free energies (kcal/mol) and electronic energies (kcal/mol, in parentheses) for the formation of **4a′**. On the basis of the calculation results, we can see that the free energy barrier for the N-end coordination process is as high as 56.4 kcal/mol and the N_2O-coordinated intermediate **4a′** is 46.8 kcal/mol higher in energy than the reactants. The high free energy barrier and instability of the intermediate with respect to the reactants indicate that the proposed mechanism is unlikely to be responsible for the formation of **2**, as the reaction of the ruthenium dihydride complex **1** with N_2O occurs at 25 °C.

(14) (a) Chen, M.; Huang, Z.; Zhou, M. *Chem. Phys. Lett.* **2004**, *384*, 165. (b) Jin, X.; Wang, G.; Zhou, M. *J. Phys. Chem. A* **2006**, *110*, 8017. (c) Yang, X.; Wang, Y.; Geng, Z.; Liu, Z. *Chem. Phys. Lett.* **2006**, *430*, 265. (d) Tishchenko, O.; Kryachko, E. S.; Vinckier, C.; Nguyen, M. T. *Chem. Phys. Lett.* **2002**, *363*, 550. (e) Tishchenko, O.; Vinckier, C.; Ceulemans, A.; Nguyen, M. T. *J. Phys. Chem. A* **2005**, *109*, 6099. (f) Karlsen, E. J.; Nygren, M. A.; Pettersson, L. G. M. *J. Phys. Chem. A* **2002**, *106*, 7868. (g) Khoroshun, D. V.; Musaev, D. G.; Morokuma, K. *Organometallics* **1999**, *18*, 5653.

(15) (a) Paulat, F.; Kuschel, T.; Nather, C.; Praneeth, V. K. K.; Sander, O.; Lehnert, N. *Inorg. Chem.* **2004**, *43*, 6979. (b) Ghosh, S.; Gorelsky, S. I.; Chen, P.; Cabrito, I.; Moura, J. J. G.; Moura, I.; Solomon, E. I. *J. Am. Chem. Soc.* **2003**, *125*, 15708. (c) Gorelsky, S. I.; Ghosh, S.; Solomon, E. I. *J. Am. Chem. Soc.* **2006**, *128*, 278.

(16) (a) Becke, A. D. *J. Chem. Phys.* **1993**, *98*, 5648. (b) Miehlich, B.; Savin, A.; Stoll, H.; Preuss, H. *Chem. Phys. Lett.* **1989**, *157*, 200. (c) Lee, C.; Yang, W.; Parr, R. G. *Phys. Rev. B* **1988**, *37*, 785. (d) Stephens, P. J.; Devlin, F. J.; Chabalowski, C. F.; Frisch, M. J. *J. Phys. Chem.* **1994**, *98*, 11623.

(17) (a) Fukui, K. *J. Phys. Chem.* **1970**, *74*, 4161. (b) Fukui, K. *Acc. Chem. Res.* **1981**, *14*, 363.

(18) Krishnan, R.; Binkley, J. S.; Seeger, R.; Pople, J. A. *J. Chem. Phys.* **1980**, *72*, 650.

(19) (a) Bergner, A.; Dolg, M.; Kuechle, W.; Stoll, H.; Preuss, H. *Mol. Phys.* **1993**, *80*, 1431. (b) Dolg, M.; Wedig, U.; Stoll, H.; Preuss, H. *J. Chem. Phys.* **1987**, *86*, 866.

(20) Ehlers, A. W.; Bohme, M.; Dapprich, S.; Gobbi, A.; Hollwarth, A.; Jonas, V.; Kohler, K. F.; Stegmann, R.; Veldkamp, A.; Frenking, G. *Chem. Phys. Lett.* **1993**, *208*, 111.

(21) (a) Barone, V.; Cossi, M. *J. Phys. Chem. A* **1998**, *102*, 1995. (b) Cossi, M.; Rega, N.; Scalmani, G.; Barone, V. *J. Comput. Chem.* **2003**, *24*, 669. (c) Tomasi, J.; Mennucci, B.; Cammi, R. *Chem. Rev.* **2005**, *105*, 2999.

(22) Schaftenaar, G. *Molden V3.7*; CAOS/CAMM Center Nijmegen: Toernooiveld, Nijmegen, The Netherlands, 2001.

(23) Frisch, M. J.; et al. *Gaussian 03, revision B05*; Gaussian, Inc.: Pittsburgh, PA, 2003.

(24) Glendening, E. D.; Reed, A. E.; Carpenter, J. E.; Weinhold, F. *NBO*, Version 3.1.

(25) (a) Reed, A. E.; Curtiss, L. A.; Weinhold, F. *Chem. Rev.* **1988**, *88*, 899. (b) Wiberg, K. B. *Tetrahedron* **1968**, *24*, 1083.

Scheme 2

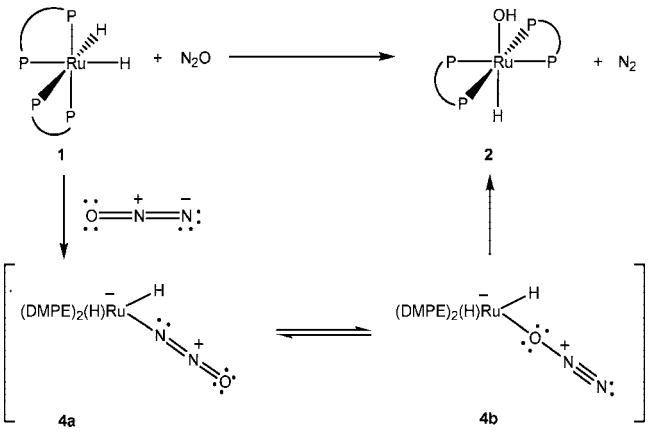

It is interesting to note that the calculated structure of the N_2O-coordinated intermediate **4a′** (Scheme 3) is different from the one proposed in Scheme 2. In the calculated structure of **4a′**, the Ru−N_2O structural moiety adopts a zigzag conformation in which the N_2O ligand can be considered as carrying a formal charge of −2 (see the Lewis structures given in Scheme 3). Through coordination, N_2O formally accepts two electrons from the metal center. An NBO population analysis on the species involved in Scheme 3 also indeed shows that there is a significant charge transfer from the ruthenium dihydride complex **1** to N_2O (the partial charges of the N_2O ligand are −0.7 in $\mathbf{TS_{(1-4a)}}$ and −1.1 in **4a′**). The bent coordinated N_2O has also been proposed in a recent theoretical study.[26]

We also attempted to obtain the O-end coordination mode as proposed in the intermediate **4b** (Scheme 2). Our calculation results show that **4b** also does not correspond to a local minimum. Nevertheless, we successfully located the transition state $\mathbf{TS_{(1-6)}}$ relevant to a direct O-insertion into one of the two Ru−H bonds (Scheme 4). The direct O-insertion gives N_2 and the cis complex **6**. The free energy barrier calculated for such a direct O-insertion is 35.3 kcal/mol, which appears to be too high for the insertion to occur under the experimental conditions.[6] Therefore, we have to investigate other possibilities so as to get a more convincing mechanism for the reaction of the dihydride complex **1** with N_2O.

Mechanism for the Formation of 2. On the basis of our DFT calculations, path II shown in Figure 1 was found to be the most favorable for formation of the monoinsertion product **2**. Figure 2 shows the optimized structures with selected structural parameters for the species involved in Figure 1. For comparison, selected structural parameters from the X-ray structure of $(dmpe)_2Ru(OH)H$ are also presented in parentheses for **2**. The calculated geometry reproduces the important experimental structural parameters quite well.

From Figure 1, we can see that the reaction $\mathbf{1} + N_2O \rightarrow \mathbf{2} + N_2$ is highly exergonic. For both paths I and II, the first step for the formation of **2** involves N_2O activation. In the activation step, N_2O approaches the hydride ligand of the ruthenium dihydride complex via the terminal nitrogen atom. A hydride transfer to N_2O occurs from the ruthenium dihydride complex **1**, leading to the formation of **5** via breaking of one Ru−H bond and coordination of the activated N_2O through the O-end. For path I, the intermediate **5** then undergoes N_2 loss with a barrier of 28.5 kcal/mol, and the relatively stable complex **6** is formed with the hydroxyl group cis to the remaining hydride. The cis complex **6** can then isomerize to the trans complex **2** via a dissociative pathway (path I, Figure 1). In the dissociative pathway, the Ru−P bond that is trans to the remaining hydride dissociates to give the five-coordinate intermediate **7** via rotating the phosphine ligand along the C−C single bond of the dmpe ligand involved. From **7**, a ligand rearrangement together with a ligand recoordination takes place with a barrier of 8.4 kcal/mol, giving the monoinsertion product **2**. The overall barrier for the formation of the monoinsertion product **2** via path I is 29.3 kcal/mol.

In view of the result that the cis-to-trans isomerization (**6** → **2**) is relatively easier than the N_2 loss process (**5** → **6**), we considered another possibility of having a cis-to-trans isomerization from **5** before the N_2 loss takes place (path II, Figure 1). The cis-to-trans isomerization from **5** to **9** follows a dissociative pathway similar to **6** → **2**. The free energy barrier (25.0 kcal/mol) for the cis-to-trans isomerization from **5** to **9** in path II is greater than that (20.1 kcal/mol) for the isomerization from **6** to **2** in path I, due to the fact that the intermediate **5** has a more crowded ligand environment than the complex **6**. However, the N_2 loss from **9** in path II has a lower free energy barrier (24.6 kcal/mol) than the N_2 loss from **5** in path I (28.5 kcal/mol). In **9**, the ONNH ligand is trans to the hydride ligand. The strong trans influence of the hydride ligand weakens the Ru−ONNH bond, making the oxygen carry a more negative charge and facilitating the proton migration and the N_2 loss. An NBO population analysis shows that the oxygen of the ONNH ligand carries a charge of −0.13 in **9** and −0.10 in **5**. The overall barrier for the formation of the monoinsertion product **2** via path II is 25.8 kcal/mol, lower than that (29.3 kcal/mol) via path I.

We also examined the possibility of ionizing the intermediate **5** into the separated ions $[Ru(dmpe)_2H]^+$ and $[ONNH]^-$, from which the cation relaxes/isomerizes to a square pyramid with an apical hydride, and then the anion deposits OH^- to give the monoinsertion product **2**. To examine the stability of the separated ion pair, we partially optimized the pair by fixing the distance at 10 Å between the metal center of the cation and the oxygen atom of the anion. In the gas phase, as expected, the separated ion pair is highly unstable, ca. 65 kcal/mol higher in free energy than the intermediate **5**. In the solution phase, the separated ion pair was calculated, with the polarizable continuum model (PCM)[21] having benzene as the solvent, to be ca. 44 cal/mol higher in free energy than the intermediate **5**. The instability of the separated ion pair suggests that the pathway via an ion pair is unlikely.

Figure 1 shows that the cis and trans complexes **6** and **2** have stability comparable with the trans complex **2**, being slightly more stable by only 0.5 kcal/mol in terms of their relative free energy. The comparable stability of the two complexes is not unexpected in view of the fact that in the literature the two different structural moieties adopted by the $Ru(dmpe)_2$ metal fragment in **2** and **6** are frequently found in bis(dmpe) complexes of Ru.[27] Experimentally, only the trans complex **2** is observed,[6] suggesting that theory might either have overestimated the stability of the cis complex **6** or have underestimated the stability of the trans complex **2** by a couple of kcal/mol. We further estimated the relative energy by employing the MPW1K method.[28] The relative free energy was calculated to increase to 1.0 kcal/mol, with the trans complex **2** being more stable.

(26) Fan, H.; Caulton, K. G. *Polyhedron* **2007**, *26*, 4731.

(27) For example:(a) Jones, W. D.; Libertini, M. *Inorg. Chem.* **1986**, *25*, 1794. (b) Fulton, J. R.; Sklenak, S.; Bouwkamp, M. W.; Bergman, R. G. *J. Am. Chem. Soc.* **2002**, *124*, 4722. (c) Kirkham, M. S.; Mahon, M. F.; Whittlesey, M. K. *Chem. Commun.* **2001**, 813. (d) Burn, M. J.; Fickes, M. G.; Hollander, F. J.; Bergman, R. G. *Organometallics* **1995**, *14*, 137.

Scheme 3

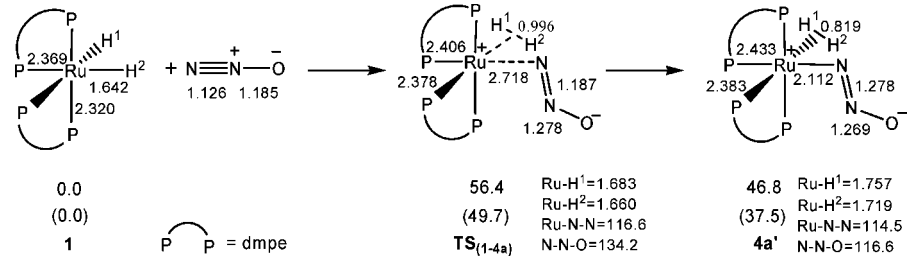

Scheme 4

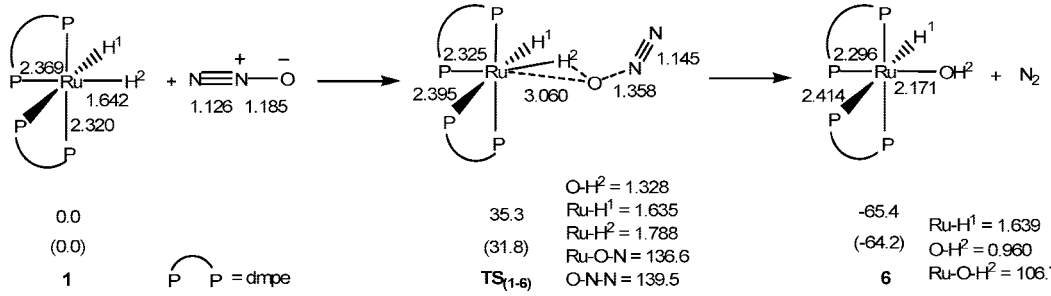

Mechanism for the Formation of 3. The mechanism of oxygen transfer from N_2O to the monoinsertion product **2**, leading to the formation of **3** (Figure 3), is similar to that from N_2O to the ruthenium dihydride **1** (**1** + N_2O → **6** + N_2, Figure 1). The optimized structures with selected structural parameters for the species involved in Figure 3 are shown in Figure 4. Similar to what we have seen above, the first step involves N_2O activation. N_2O approaches the hydride ligand via the N-end, giving **10** via breaking of the Ru−H bond and coordination of the activated N_2O through the O-end. Without the need for isomerization, **10** then undergoes the N_2 loss process with a free energy barrier of 23.9 kcal/mol and the bis(hydroxo) complex $(dmpe)_2Ru(OH)_2$ (**3**) is formed. The overall free energy barrier for formation of the bis(hydroxo) complex **3** from the monoinsertion product **2** is 27.0 kcal/mol.

The overall free energy barrier for the second oxygen transfer (**2** → **3**) is slightly higher than that for the first oxygen transfer (**1** → **2**). The slightly less favorable second oxygen transfer implies that when the bis(hydroxo) complex **3** is directly synthesized from the ruthenium dihydride **1**, the overall barrier should be equal to that for the formation of **3** from **2**. The results are consistent with the experimental observation that treatment of either the ruthenium dihydride **1** or the isolated monoinsertion product **2** with an atmosphere of N_2O under the same conditions afforded the bis(hydroxo) complex **3** in the same yield.[6]

Other Possible N_2O Activation Modes. As discussed above, the most favorable mode for activation of N_2O involves a direct attack on the terminal nitrogen from one of the Ru−H bonds via $\mathbf{TS_{(1-5)}}$. There is also a possibility that a dissociative mechanism operates in which one of the Ru−P bonds dissociates

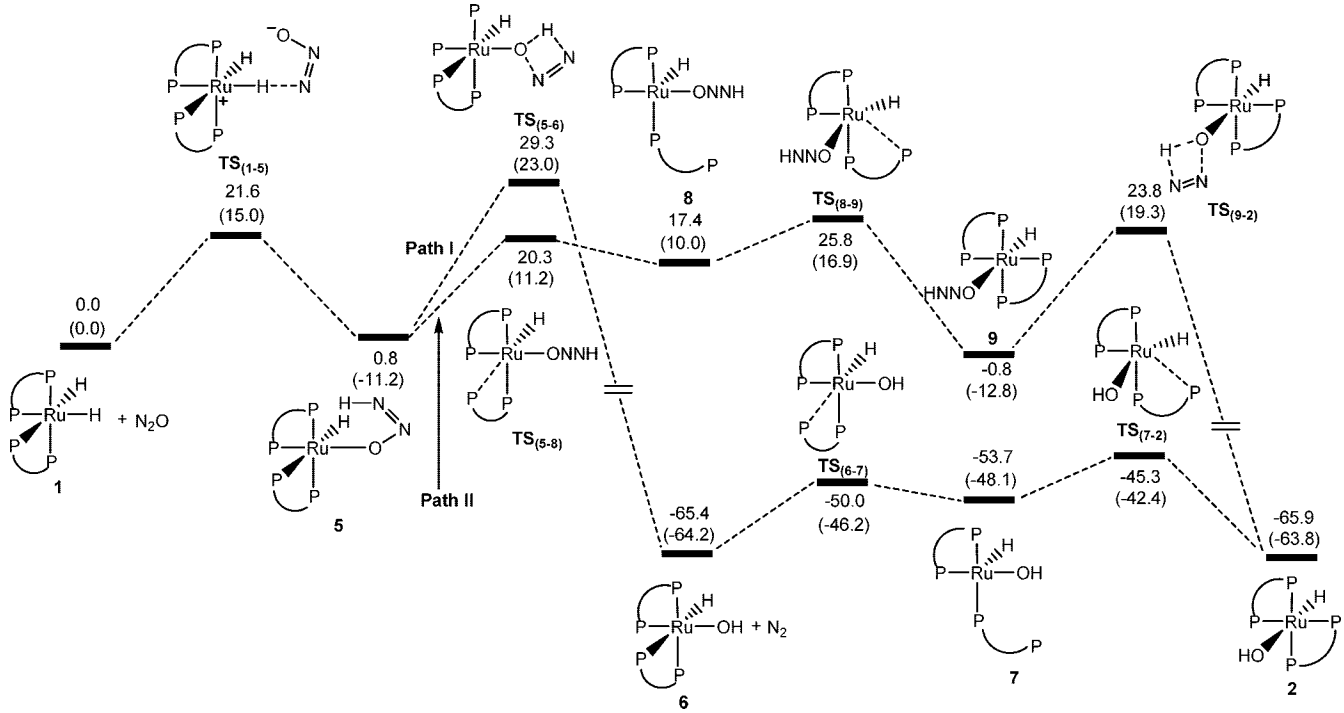

Figure 1. Energy profiles calculated for the formation of the monoinsertion product **2** from the reaction of $(dmpe)_2RuH_2$ (**1**) with N_2O. The relative free energies and electronic energies (in parentheses) are given in kcal/mol.

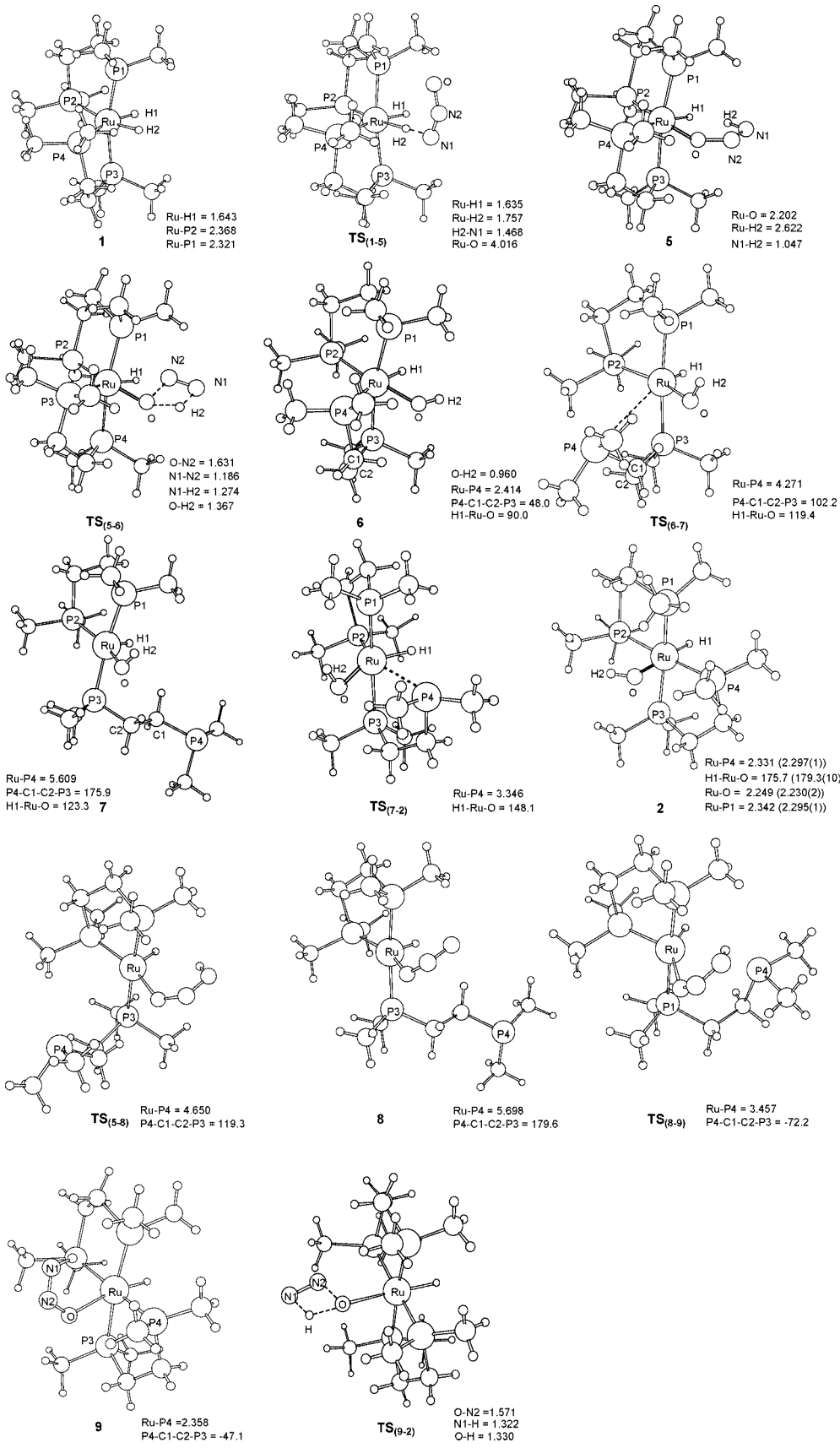

Figure 2. Optimized structures with selected structural parameters for species shown in Figure 1. The bond distances and angles are given in Å and deg, respectively.

first to provide a vacant site on the metal center for coordination of N_2O. The energetics associated with this possible mechanism is shown in Figure 5. Dissociation of one of the Ru−P bonds takes place with the formation of the five-coordinated, 16-electron ruthenium intermediate **11**. The barrier for the dissociation step is 28.1 kcal/mol, and **11** is 23.2 kcal/mol higher

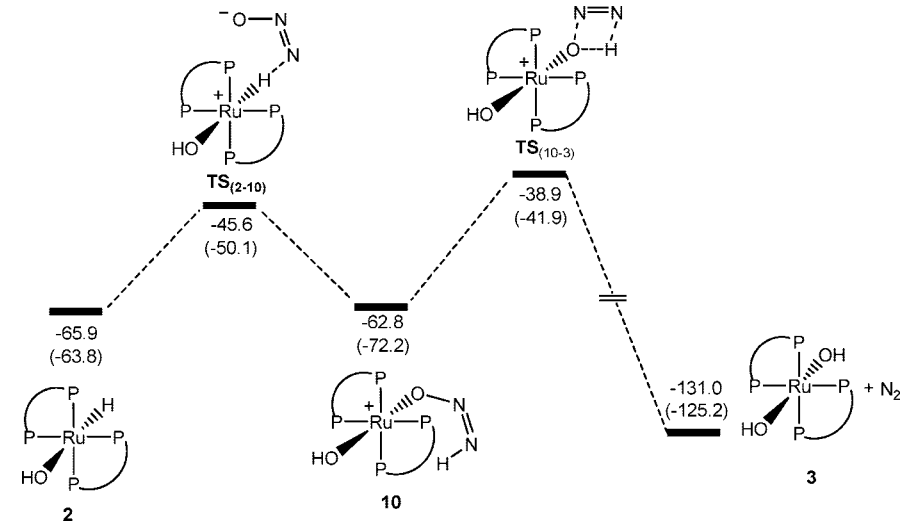

Figure 3. Energy profiles calculated for the formation of the bis(hydroxo) complex **3** from the reaction of $(dmpe)_2RuH(OH)$ (**2**) with N_2O. The relative free energies and electronic energies (in parentheses) are given in kcal/mol.

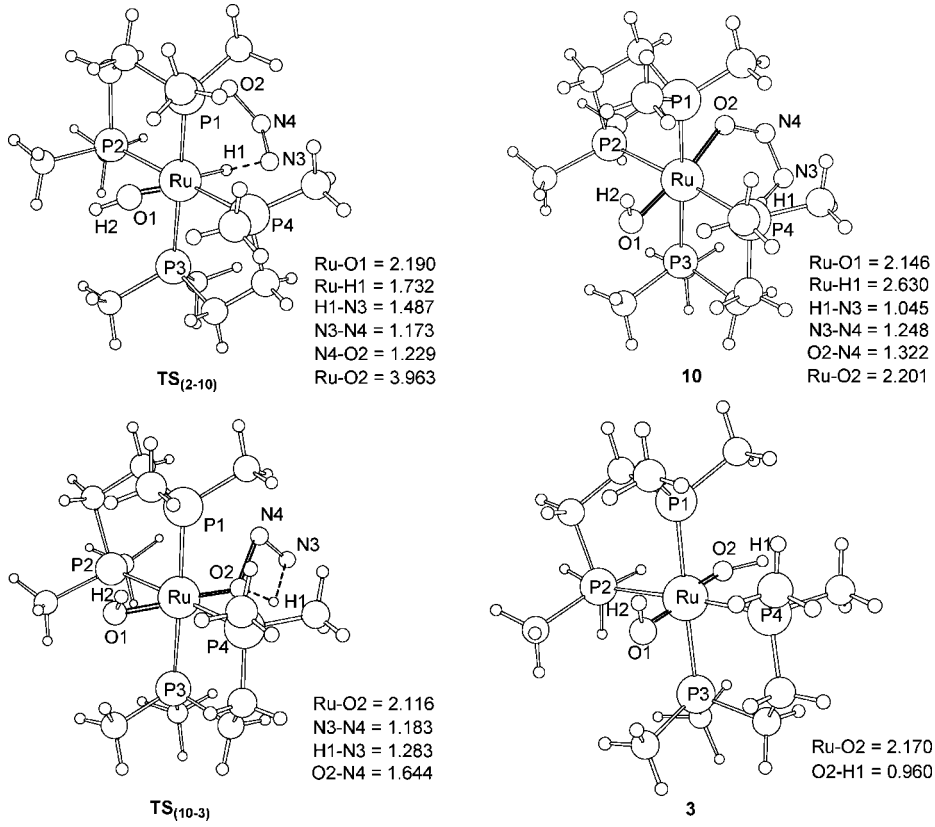

Figure 4. Optimized structures with selected structural parameters for species shown in Figure 3. The bond distances and angles are given in Å and deg, respectively.

in free energy than the reactant **1**. Here, we noticed that the loss of one P from a P chelate is more costly for the $[Ru](H)_2$ ($[Ru] = (dmpe)_2Ru$) species **1** (Figure 5) than for the [Ru](ONNH)(H)/[Ru](OH)(H) species **5/6** (Figure 1). This is caused by the "cis effect", for which a π donation from the lone pair on the oxygen atom stabilizes the unsaturated transition states.[29] From **11**, coordination of N_2O to the vacant site on the metal center can occur either via the N-end (Figure 5a) or via the O-end (Figure 5b). In Figure 5a, the N-end-coordinated intermediate **12** then undergoes an intramolecular hydride transfer to form the intermediate **13** via the transition state $\mathbf{TS_{(12-13)}}$. In Figure 5b, the O-end-coordinated intermediate **14** lies ca. 10 kcal/mol higher in free energy than the N-end-coordinated intermediate **12** and undergoes a hydride transfer to form the intermediate **15** via the transition state $\mathbf{TS_{(14-15)}}$. The overall barriers leading to the formation of the intermediates **13** and **15** are 39.4 and 43.4 kcal/mol, respectively, both of which are much higher in free energy than the overall N_2O activation

(28) Lynch, B. J.; Fast, P. L.; Harris, M.; Truhlar, D. G. *J. Phys. Chem. A* **2000**, *104*, 21.
(29) Jordan, R. B. *Reaction Mechanisms of Inorganic and Organometallic Systems*; New York: Oxford University Press, 1998.

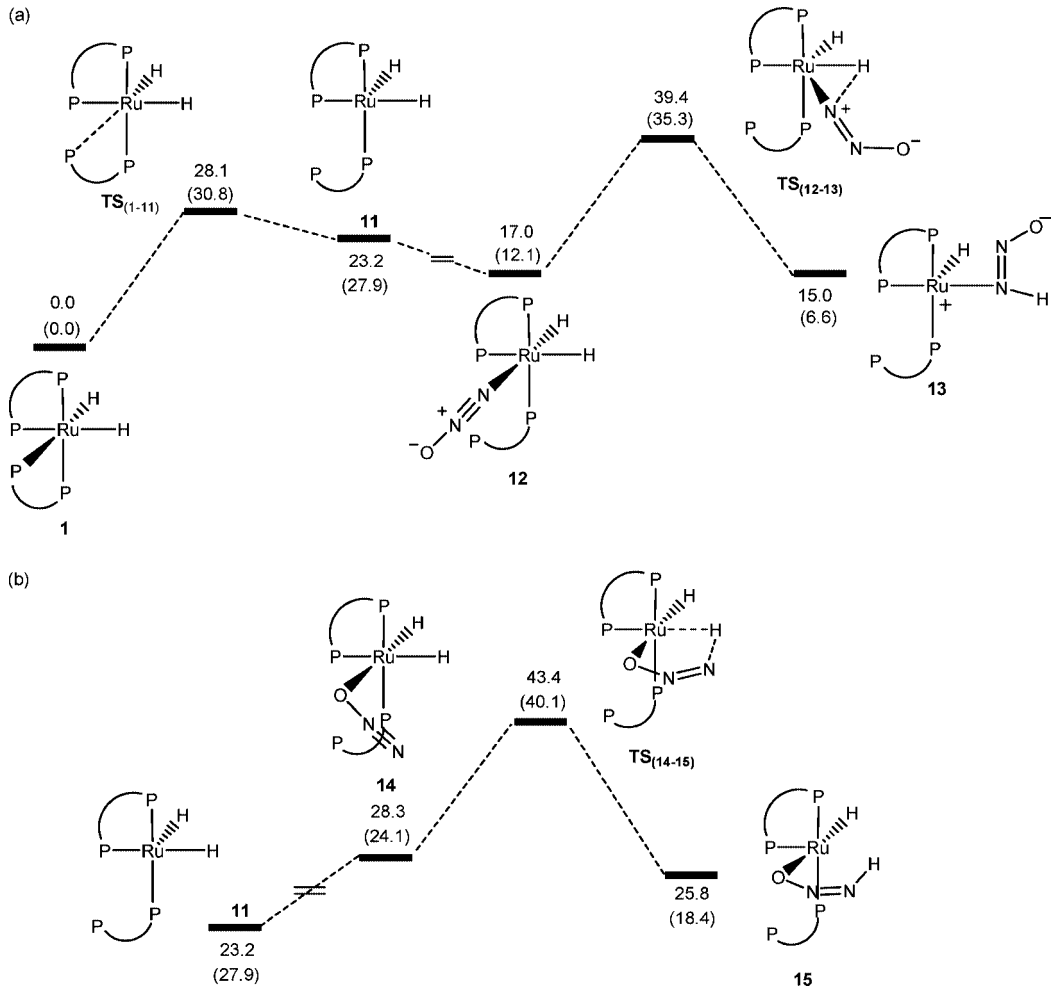

Figure 5. Energy profiles calculated for the formation of the monoinsertion product **2** through a dissociative pathway via N-coordination (a) and O-coordination (b) of N_2O. The relative free energies and electronic energies (in parentheses) are given in kcal/mol.

barrier for the formation of **2** or **3** via the pathways shown in Figures 1 and 3. The large ligand dissociation energy together with the extremely poor coordination ability of N_2O is responsible for the substantially high overall barriers for the dissociative pathways.

We also considered other possible modes for activation of N_2O (Scheme 5). One possibility is that one of the Ru−H bonds attacks directly the terminal oxygen of N_2O to form the intermediate **16** via breaking of the Ru−H bond followed by coordination of the activated N_2O through the N-end (eq 1 in Scheme 5). Our calculation results show that the free energy barrier for such an activation mode is 31.3 kcal/mol, ca. 4 kcal/mol higher in free energy than the overall barrier for the formation of **2** or **3** via the pathways shown in Figures 1 and 3. Interestingly, the expected intermediate **16** does not correspond to a local minimum, and optimization of structure **16** led to an ion pair of the dinitrogen-coordinated cationic complex **20** and the anion OH^-. The energetics associated with the ion pair shown in Scheme 5 were approximate because it is known that DFT is not suitable for modeling such an ion pair. The instability of the −N=N−OH ligand in the structure **16** is likely due to nonbonded lone pair−lone pair repulsions between the directly bonded N and O atoms. A supporting evidence for this argument is that optimization of the anion $[N{=}N{-}OH]^-$ results in the N−O bond breaking and gives N_2 and OH^-.

N_2O could also be activated with the modes shown in eqs 2, 3, or 4 of Scheme 5. The calculation results (Scheme 5) show that the free energy barriers for all these activation modes are much higher than the overall barrier for the formation of **2** or **3** via the pathways shown in Figures 1 and 3.

Insight into the N_2O Activation. Having gained the mechanistic details for the formation of the monoinsertion product **2** and the bis(hydroxo) complex **3**, we then investigated how the kinetically inert N_2O is activated during the reaction of the ruthenium dihydride complex **1** with N_2O. We first examined the frontier orbitals calculated for N_2O and the ruthenium dihydride complex **1**. As shown in Figure 6, the HOMOs of N_2O can be considered as nonbonding and the LUMOs are antibonding among the three atoms. For the ruthenium dihydride complex **1**, the HOMO, HOMO−1, and HOMO−2 are the nonbonding t_{2g} orbitals localized on the ruthenium center. Immediately below the t_{2g} orbitals is the bonding orbital HOMO−3 of the Ru−H bonds in the ruthenium dihydride complex **1**. Structurally, we have seen that N_2O is activated by its interaction with one of the hydride ligands of **1**. Thus, the orbital associated with the Ru−H bonds is important. In Figure 6, we can see that the energy gaps between the LUMOs of N_2O and the HOMO−3 of the ruthenium dihydride complex **1** are much smaller than those between the HOMOs of N_2O and the LUMO of the ruthenium dihydride complexes. Therefore, N_2O is expected to be best activated through the orbital interactions between the HOMO−3 of the ruthenium dihydride complexe **1** and the LUMOs of N_2O.

Scheme 5

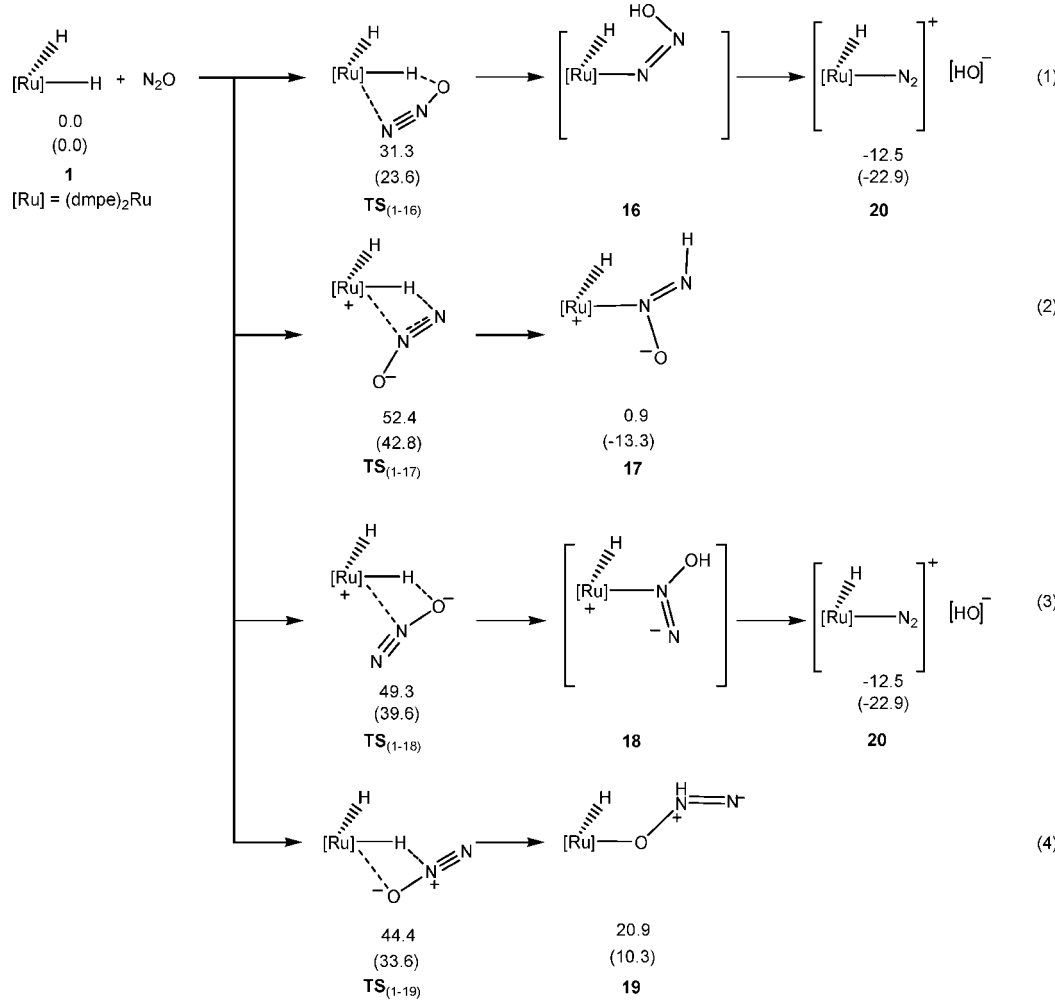

In the N_2O activation transition state $\mathbf{TS_{(1-5)}}$ (Figure 2), the hydride transfer from the dihydride complex **1** to N_2O can be seen clearly with the H(2)−N(1) distance being as short as 1.468 Å. The HOMO−3 of the dihydride complex **1** corresponds to the Ru−H bonding orbital and is mainly localized on the hydride ligands. The spherical property of the 1s orbitals of the two hydride ligands makes the hydride ligands vulnerable to attack by external electrophiles. In other words, the hydride ligands act as nucleophiles and nucleophilically attack the N-end of N_2O. On the basis of the orbital analysis above and the structure of $\mathbf{TS_{(1-5)}}$, one can envisage the activation process as follows. One of the hydride ligands in the ruthenium dihydride complex **1** nucleophilically attacks the N-end of N_2O, causing rearrangement of the electron pairs associated with the N_2O moiety to achieve the transition state $\mathbf{TS_{(1-5)}}$ with a dangling O^- and a cationic ruthenium center. After the transition state is achieved, Ru−O bond formation takes place easily to form the intermediate **5** (Scheme 6). An NBO population analysis on the species involved in the N_2O activation processes (**1** → **5**) also shows that there is significant electron transfer from the ruthenium dihydride complex **1** to N_2O (the natural populations of the N_2O moiety are −0.4 in $\mathbf{TS_{(1-5)}}$ and −1.0 in **5**). The idea that hydride is a nucleophile has also been proposed in the work of

Scheme 6

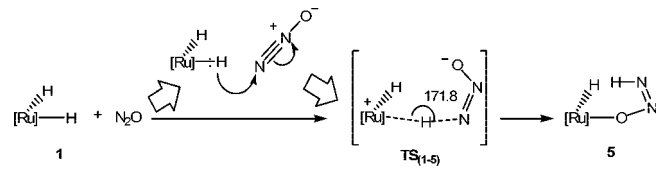

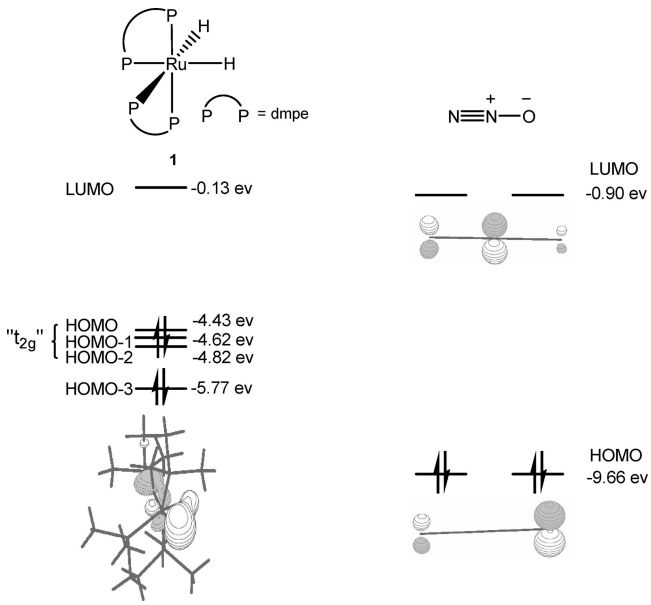

Figure 6. Frontier molecular orbitals calculated for $(dmpe)_2RuH_2$ (**1**) and N_2O.

Darensbourg et al. on the reaction of $HW(CO)_5^-$ with CO_2 to give formate.[30]

The free energy barriers calculated for the N_2O activation modes shown in Scheme 5 are all higher than the overall free energy barriers shown in Figures 1 and 3. For eq 1, N_2O is activated through one of the hydride ligands nucleophilically attacking the terminal oxygen of N_2O. As shown in Figure 6, the LUMOs of N_2O mainly consist of π^* orbitals from the two nitrogen atoms. Therefore, optimal orbital overlap cannot be achieved for this activation mode through the interaction between one of the hydride ligands and the terminal O atom of N_2O. The activation barriers calculated for the two modes shown in eqs 2 and 3 are much greater than that for the mode shown in eq 1. The results are likely due to the formation of a dangling O^- (in eq 2) or N^- (in eq 3) and a steric reason that prevents the effective formation of an Ru−N bond between the ruthenium center and the central nitrogen atom of N_2O. The activation mode in eq 4 involves a hydride transfer to the central nitrogen followed by formation of a Ru−O bond. The activation barrier for this mode is also very high (44.4 kcal/mol), and the intermediate **19** formed from this mode is very unstable. The results seem unexpected because hydride attack on the LUMO of N_2O should preferentially occur at the central N, as is evident in Figure 6. Clearly, the high barrier for this mode can also be attributed to the formation of a species that has a formally minus charge on the dangling (terminal) nitrogen (see $\mathbf{TS_{(1-19)}}$ and the intermediate **19** in eq 4 of Scheme 5).

(30) (a) Darensbourg, D. J.; Jones, M. L. M.; Reibenspies, J. H. *Inorg. Chem.* **1993**, *32*, 4675. (b) Darensbourg, D. J.; Joyce, J. A.; Rheingold, A. *Organometallics* **1991**, *10*, 3407. (c) Darensbourg, D. J.; Pala, M. *J. Am. Chem. Soc.* **1985**, *107*, 5687. (d) Darensbourg, D. J.; Meckfessel Jones, M. L.; Reibenspies, J. H. *Inorg. Chem.* **1996**, *35*, 4406.

Conclusion

The detailed mechanisms for the formation of the monoinsertion product **2** and the bis(hydroxo) complex **3** from the reaction between N_2O and the ruthenium dihydride complex $(dmpe)_2Ru(H)_2$ (**1**) have been investigated with the aid of DFT calculations. We studied various activation modes for the kinetically inert N_2O and found that without metal coordination, N_2O is directly activated through the hydride ligand nucleophilically attacking its terminal nitrogen followed by coordination of the activated N_2O via the O-end. The orbital interactions involved are between the highest occupied Ru−H bonding orbital of the ruthenium dihydride complex **1** and the unoccupied π^* orbitals of N_2O. The spherical property of the 1s orbitals of the two hydride ligands allows the hydride ligands to be vulnerable to attack by N_2O, an external electrophile. Consistent with the conclusion made from our previous work, highly electron-rich species are needed for the N_2O activation.

Acknowledgment. This work is supported by the Hong Kong University of Science and Technology through grants CA-MG06/07.SC01, CA-MG07/08.SC03, and RPC06/07.SC09.

Supporting Information Available: Complete ref 23, tables giving Cartesian coordinates and electronic energies for all of the calculated structures. This material is available free of charge via the Internet at http://pubs.acs.org.

OM8000845